

Experimental Study of the Miniaturized Cylindrical Rotating Detonation Engine

Karin Hattori¹, Kosei Ota¹, Kazuki Ishihara¹, Keisuke Goto¹, Noboru Itouyama¹,
Hiroaki Watanabe¹, Akira Kawasaki¹, Ken Matsuoka¹, Jiro Kasahara¹,
Akiko Matsuo², Ikkoh Funaki³

1 Nagoya University, Chikusa-ku, Nagoya, Aichi, Japan

2 Keio University, Kohoku-ku, Yokohama, Kanagawa, Japan

3 JAXA Institute of Space and Astronautical Science, Chuo-ku, Sagamihara, Kanagawa, Japan

1 Introduction

A detonation wave is a self-sustained combustion wave that propagates at supersonic speed. Comparing the detonation and deflagration combustion, detonation combustion is characterized by theoretically higher thermal efficiency than the Brayton cycle, which is a common internal combustion engine cycle, because detonation combustion occurs at higher temperatures and pressures [1-4]. Furthermore, the combustion process in detonation combustion is completed in a very short time due to the passage of supersonic combustion waves. Therefore, the engine using detonation combustion has the potential to realize a smaller combustor with higher thermal efficiency [4-7]. Various types of detonation engines have been proposed, such as the Pulse Detonation Engine (PDE) and the Rotating Detonation Engine (RDE), due to differences in the propagation of detonation waves.

Among them, RDEs typically have a double-cylinder combustor, and thrust is generated by detonation waves rotating circumferentially in its channels. As a result, the combustion in an RDE is continuous, and the thrust density is usually higher than that of a PDE, which generates pulsed combustion [8]. In particular, the inner cylinder of the combustor of RDE is subjected to a high heat load during combustion and account for a considerable amount of the structural weight of the entire RDE. In recent years, a single-cylinder RDE without the inner cylinder has been studied numerically and experimentally, and its feasibility has been demonstrated [8-12]. More recently, a propellant injection mechanism has been proposed in which the propellant injector is placed on the outer wall of the combustion chamber of a cylindrical RDE to cool the side walls of the combustor [13]. A cylindrical RDE which has both compact and high-performance is becoming a reality.

Here, it is important to know how far the size of the combustor can be reduced. In recent years, innovations in manufacturing technology have made it possible to manufacture complex shapes by additive manufacturing (AM) in addition to conventional cutting and welding [13]. To use AM in the manufacture of combustors allows the incorporation of the cooling mechanism described above, as well as increasing the flexibility of the combustor shape. However, no RDE combustor with a bottom shape

different from a flat bottom has been designed or demonstrated, and the flexibility of the RDE combustor shape has not been verified.

One of the problems that arises when combustors are made smaller is that the effective combustion cross-sectional area becomes smaller due to the developed boundary layer. This is because the smaller the size, the smaller the ratio of volume per area. In other words, when considering downsizing, it is necessary to evaluate the effect of the boundary layer on the combustion cross-sectional area.

In this study, we fabricated and tested an RDE combustor with a spherical bottom shape as well as a planar bottom shape and a cooling mechanism, taking advantage of the characteristics of AM. Also, these were smaller than conventional ones to evaluate the effect of the boundary layer.

2 Experimental Methods

Figure 1 shows an overview of the two types of cylindrical RDE combustors fabricated in this study. These combustors are made of stainless steel and aluminum parts for pressure resistance and workability. Fluoroplastic O-rings are used to seal each part. The length of the combustion chamber is 75 mm and the inner diameter is 16 mm. The combustion chamber length is based on the conventional small single cylinder RDE [8], and the inner diameter is further reduced to make it more compact. The pressure ports are located at the position shown in Figure 1, and is measured by a pressure transducer (Keller: PAA-23) with a measurement frequency of 1 kHz. There are eight plenum chambers, four for fuel and four for oxidizer, and each plenum chamber supplies propellant to the combustion chamber from the bottom and sides through a fine-hole injector. Each plenum chamber supplies propellant to the combustion chamber from the bottom and sides through fine-hole injectors.

The two types of combustors have different bottom shapes and be referred to as cylindrical combustors (Figure 1a) and spherical bottom combustors (Figure 1b). Though the spherical-bottomed combustor is more difficult to manufacture, it is expected to have two structural advantages over the cylindrical-bottomed combustor: (1) the spherical-bottomed combustor has a smoother connection between the bottom and the wall of the combustor, which avoids stress concentration, and (2) the surface area inside the combustion chamber is smaller by πr^2 , which results in a smaller heat load area.

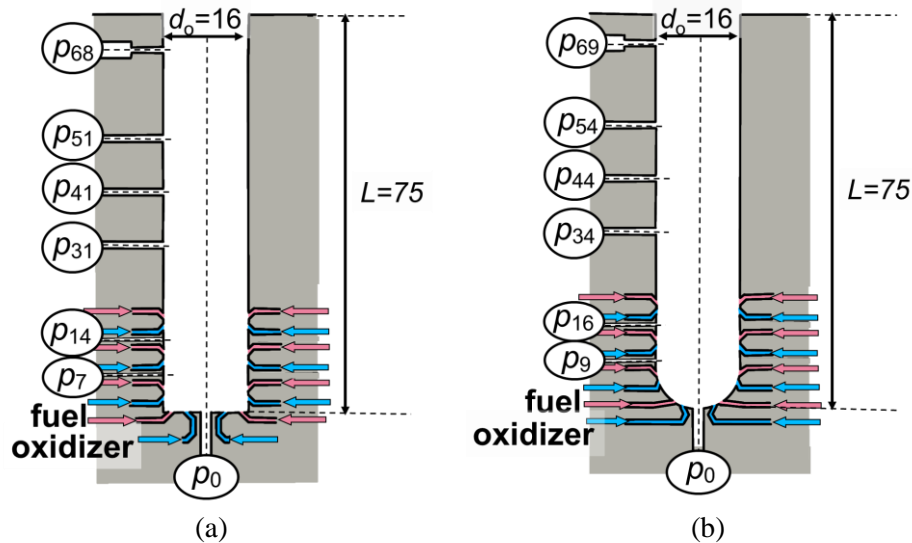


Figure 1: Cross-sections of the entire RDE (a) the cross-sectional RDE with cylindrical bottom (b) the cross-sectional RDE with spherical bottom

3 Results of Experiment

Experiments were carried out under the conditions shown in Table 1. Gaseous ethylene was used as fuel and gaseous oxygen as oxidizer, and combustion time was set to 0.5 s for safety reasons. Two types of bottom shapes, cylindrical and spherical, were burned at similar flow rates to investigate the effect of propulsion performance.

Table 1: Experimental conditions

test	Bottom shape	Mass flow rate, g/s	Equivalent ratio	Back pressure, kPa	Combustion pressure, kPa	Thrust, N
1	cylindrical	12.7	1.82	10.7	115	23
2	cylindrical	27.8	1.64	10.1	257	56
3	cylindrical	35.2	1.53	9.7	329	77
4	spherical	13.6	1.77	8.7	112	21
5	spherical	25.0	1.51	9.2	214	48
6	spherical	36.6	1.56	8.8	329	73

In the following, we will discuss the boundary layer at the outlet surface. Figure 2 is a photograph of the outlet surface of a combustion experiment conducted in a cylindrical combustor at a mass flow rate of 10 g/s. The measured combustor outlet diameter is d_e , the combustion diameter of the plume is $d_{e,eff}$, and the boundary layer thickness is δ . The combustor cross-sectional area and the combustion cross-sectional area obtained from the observation of the plume are A_e and $A_{e,eff}$, respectively.

As shown in Figure 3, we measured the cross-sectional area of the combustion chamber and the cross-sectional area of the actual combustion, $A_{e,eff}/A_e$ was 0.75~0.85 and the boundary layer thickness δ was about 0.7~1.1 mm. In addition, there was no effect on the boundary layer between the cylindrical bottom and spherical bottom.

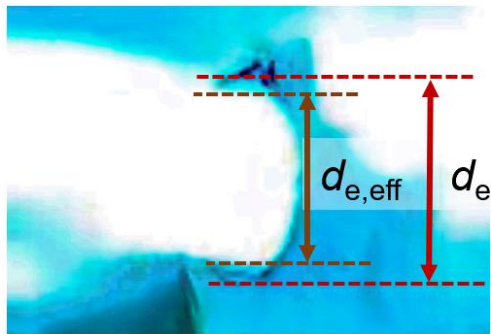


Figure 2: Images of exhaust plume

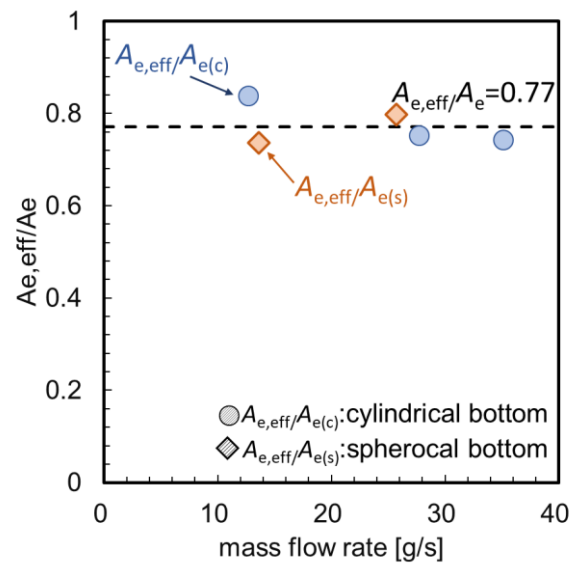


Figure 3: Results of boundary layer visualization

The theoretical values of the burnup pressure and thrust are derived using the cross-sectional area of combustion, $A_{e,eff}$, including δ , the thickness of the boundary layer. The values were obtained by replacing A_e with $A_{e,eff}$ in the equations (1) and (2) for calculating combustion pressure and thrust (Fig.4.).

$$p_c = \frac{\dot{m}\sqrt{RT_c}}{A_e \sqrt{\gamma \left(\frac{2}{\gamma+1}\right)^{\frac{\gamma+1}{\gamma-1}}}} \quad (1)$$

$$F = A_c p_c \sqrt{\frac{2\gamma^2}{\gamma-1} \left(\frac{2}{\gamma+1}\right)^{\frac{\gamma+1}{\gamma-1}} \left\{1 - \left(\frac{p_{exi}}{p_c}\right)^{\frac{\gamma-1}{\gamma}}\right\}} + A_e (p_{exi} - p_b) \quad (2)$$

Figure 4 shows graphs comparing the theoretical and measured values of combustion pressure and thrust. From these graphs, it can be predicted that both the combustion pressure and thrust will be about the same as the measured values at $A_{e,eff}/A_e = 0.7\sim 0.9$, and will converge to $A_{e,eff}/A_e = 0.8$ as the mass flow rate increases.

Furthermore, the similar values of combustion pressure and thrust for the two bottom shapes, cylindrical and spherical, suggest that the effect of bottom shape on propulsive performance is negligible.

From the above, the validity of the boundary layer thickness can be confirmed for the combustor created in this study, and the propulsive performance of the compact cylindrical RDE, regardless of the bottom shape, can be easily predicted by considering the development of the boundary layer.

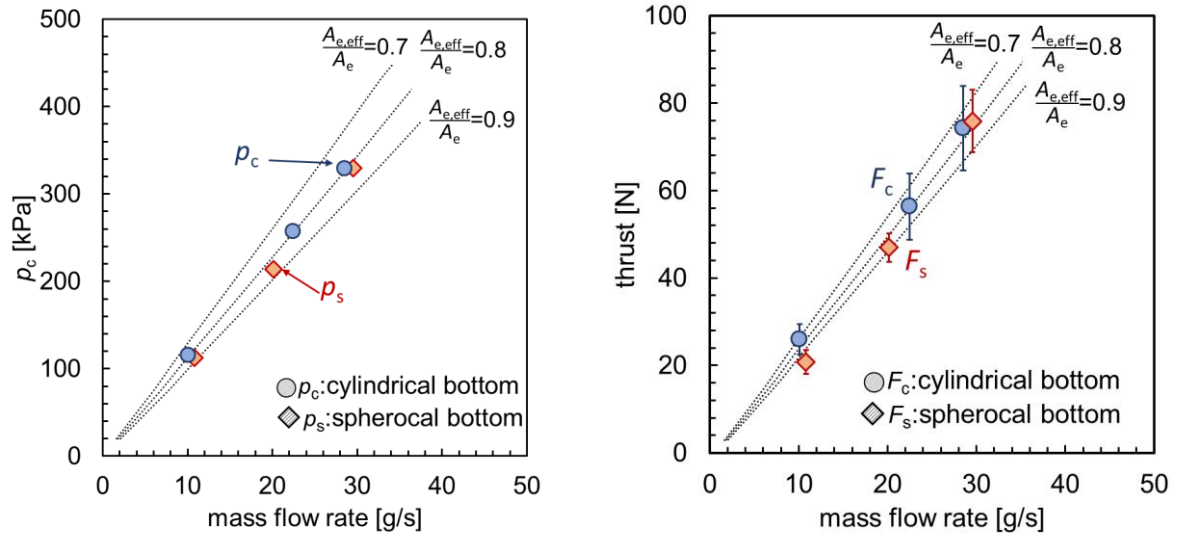


Figure 4: Comparing the theoretical and measured values of combustion pressure and thrust

4 Conclusions

A small combustor with an inner diameter of 16mm and a different bottom shape was fabricated, and the combustion cross-sectional area considering the boundary layer at the outlet surface was measured from the appearance during combustion. As a result, there was no difference in combustion due to the shape of the bottom, and the ratio of the cross-sectional area of combustion to the cross-sectional area of the combustor, $A_{e,eff}/A_e$, was 0.75~0.85. The cross-sectional area of combustion including the thickness of the boundary layer was substituted into the theoretical values of combustion pressure and thrust, and the validity was confirmed with $A_{e,eff}/A_e$ was 0.8.

Acknowledgments

This study was subsidized by a “Study on Innovative Detonation Propulsion Mechanism”, Research and Development Grant Program (Engineering) from the Institute of Space and Astronautical Science, the Aerospace Exploration Agency, by a Grant-in-Aid for Specially Promoted Research (No.19H05464), and by a “Research and Development of an Ultra-High-Thermal-Efficiency Rotating Detonation Engine with Self-Compression Mechanism,” Advanced Research Program for Energy and Environmental Technologies, the New Energy and Industrial Technology Development Organization.

References

- [1] Fickett, W., and Davis, W. C. (2000). Detonation: Theory and Experiment, Dover Publications, New York, Chaps. 2, 3.
- [2] Lee, J. H. S. (2008). The Detonation Phenomenon, Cambridge University Press, Cambridge, Chaps. 1, 4.
- [3] Law, C. K. (2006). Combustion Physics, Cambridge University Press, Cambridge, Chaps. 7, 14.
- [4] Wolanski, P. (2013). “Detonative Propulsion,” Proceedings of the Combustion Institute, Vol. 34, No.1, pp. 125-158.
- [5] Kailasanath, K. (2000). “Review of Propulsive Applications of Detonation Waves,” AIAA Journal, Vol. 38, No. 9, pp. 1698–1708.
- [6] Lu, F. K., and Braun, E. M. (2014). "Rotating Detonation Wave Propulsion: Experimental Challenges, Modeling, and Engine Concepts," Journal of Propulsion and Power, Vol. 30, No. 5, pp. 1125-1142.
- [7] Li, J. M., Teo, C. J., Khoo, B. C., Yao, S., and Wang, C. (2018). Detonation Control for Propulsion Pulse Detonation and Rotating Detonation Engines, Springer, Cham, Switzerland, Chaps. 1, 4, 8.
- [8] Yokoo, R., Goto, K., Kim, J., Kawasaki, A., Matsuoka, K., Kasahara, J., Matsuo, A., Funaki, I. (2019). “Propulsion Performance of Cylindrical Rotating Detonation Engine,” AIAA Journal, Volume 58, No.12, 2020
- [9] W. A. Stoddard and E. J. Gutmark. (2015). “Numerical Investigation of Centerbodiless RDE Design Variations,” 53rd AIAA Aerospace Sciences Meeting, AIAA 2015-0876, Kissimmee, Florida, USA, 5-9
- [10] W. A. Stoddard, et al. (2016). “Experimental Validation of Expanded Centerbodiless RDE Design,” 54th AIAA Aerospace Sciences Meeting, AIAA 2016-0128, San Diego, California, USA,
- [11] V. Anand, A. St. George, and E. Gutmark. (2016). “Hollow Rotating Detonation Combustor,” 54th AIAA Aerospace Sciences Meeting, AIAA 2016-0124, San Diego, California, USA,

- [12] Kawasaki, A., Inakawa, T., Kasahara, J., Goto, K., Matsuoka, K., Matsuo, A., and Funaki, I. (2019). "Critical Condition of Inner Cylinder Radius for Sustaining Rotating Detonation Waves in Rotating Detonation Engine Thruster," Proceedings of the Combustion Institute, Vol. 37, No. 3, pp. 3461-3469.
- [13] K. Goto, K. Ota, A. Kawasaki, H. Watanabe, N. Itouyama, K. Matsuoka, J. Kasahara, A. Matsuo, I. Funaki. (2020). "Cylindrical rotating detonation engine cooling by means of propellant injection", AIAA Propulsion and Energy 2020 Forum,